physchem

MDPI

Supplementary Materials

for

Measurement Precision and Thermal and Absorption Properties of Nanostructures in Aqueous Solutions by Transient and Steady-State Thermal-Lens Spectrometry

Vladislav R. Khabibullin,[1] Liliya O. Usoltseva,[1] Polina A. Galkina,[1] Viktoriya R. Galimova,[1] Dmitry S. Volkov,[1] Ivan V. Mikheev,[1]* and Mikhail A Proskurnin[1]*

Analytical Chemistry Division, Chemistry Department, M.V. Lomonosov Moscow State University, d. 1, str. 3, Lenin Hills, Moscow, GSP-1 V-234, 119991, Russia

* Correspondence: mikheev.ivan@gmail.com; (I.V.M.); proskurnin@gmail.com (M.A.P.); Tel.: +7-495-939-15-68 (I.V.M.).

Table of contents

Figures

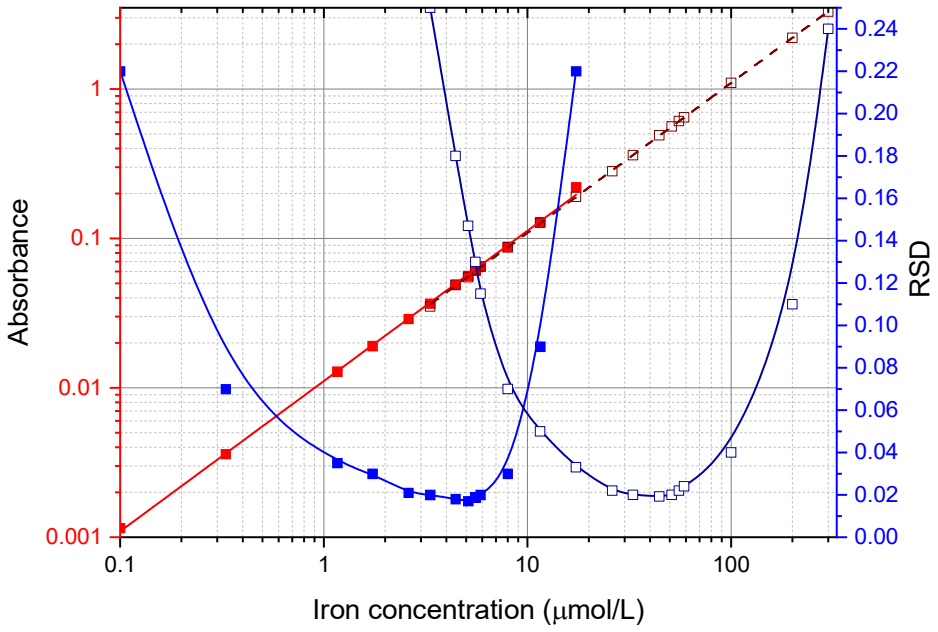

Figure S1. The linear calibration ranges of absorbance (red lines, straight; correspond to the left log-scale Y-axis) and experimental RSDs of measurements (blue lines, splined; correspond to the right linear Y-axis) for iron(II) tris(1,10-phenanthrolinate) by thermal lensing (light color curves) recalculated to absorbance and optical absorption measurements (dark-color curves) [1].

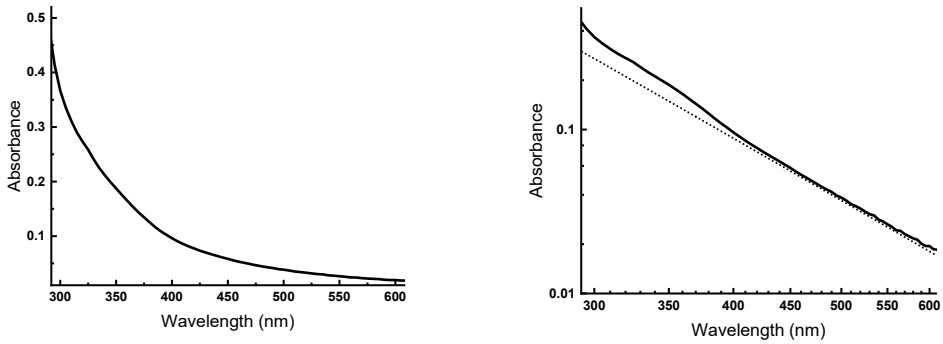

Figure S2. Absorption spectrum of colloidal silicon oxide of the AM grade, 3.2 vol.%, l = 10.0 mm. Spectra are presented in the usual coordinates (left) and in the bilogarithmic coordinates (on the right, the strokes depict the Rayleigh scattering λ^{-4}).

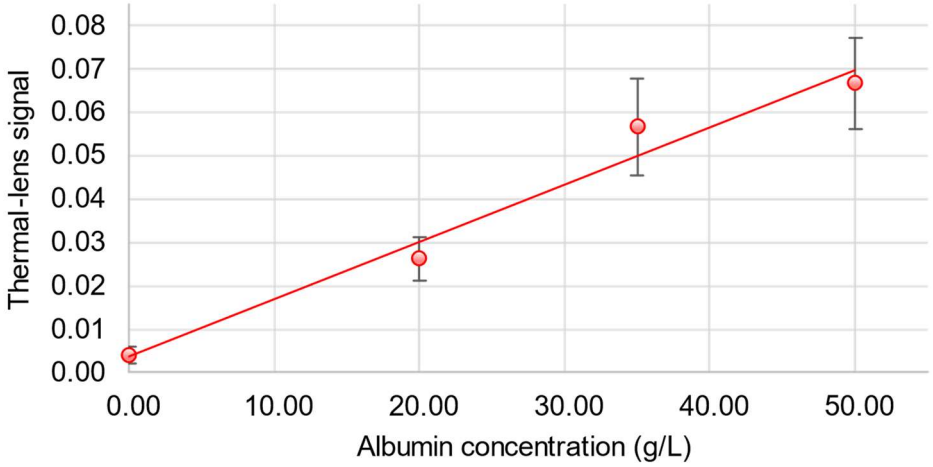

Figure S3. Dependence of the thermal lens signal on the concentration of albumin in the solution of 0.9% NaCl; Setup, TLS-60; excitation wavelength, 514.5 nm; excitation power, 40 mW.

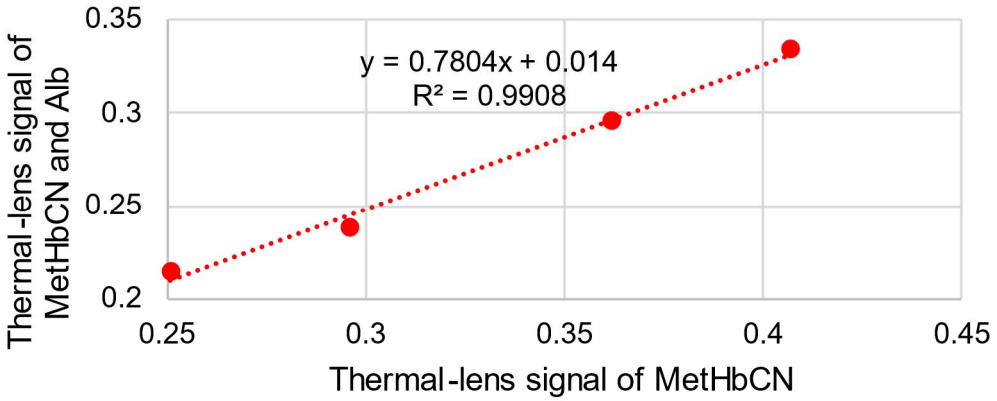

Figure S4. Correlation of the thermal-lens signal of mixtures of hemoglobin cyanide and albumin on the sum of thermal-lens signals of their individual solutions with the same concentrations. Setup, TLS-300; excitation wavelength, 445 nm; excitation power, 69 mW.

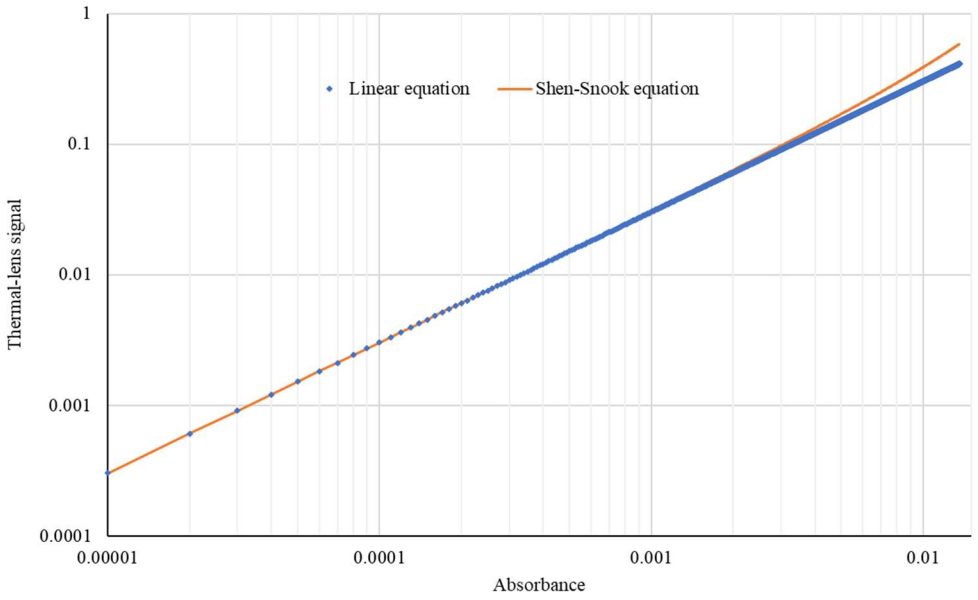

Figure S5. Log-log plot of the thermal-lens signal calculated by the linear model, Eq. (3) and Shen–Snook equation, Eq. (2), on sample absorbance, water. Setup, TLS-60; Geometry constant *B*, Eq. (4), 0.72; Excitation power, 200 mW.

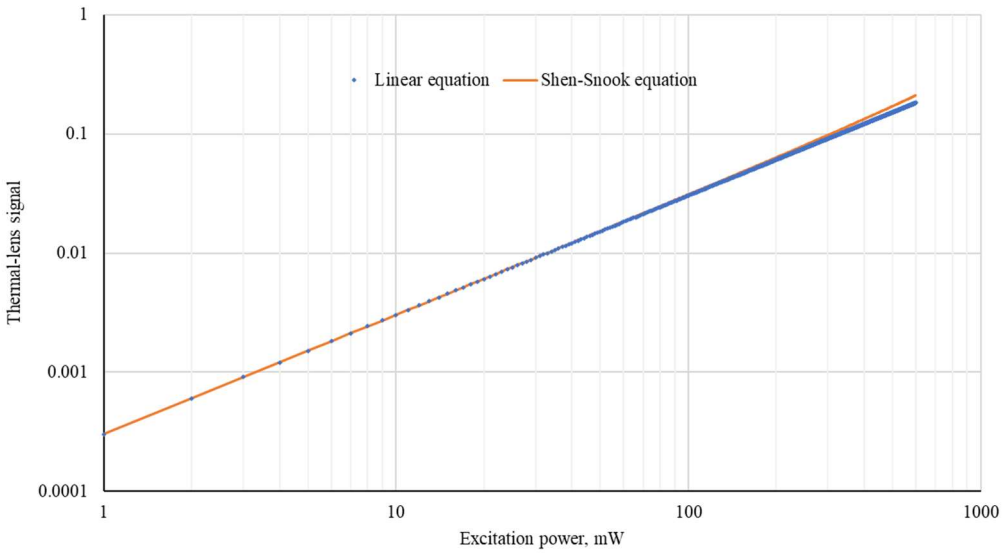

Figure S6. Log-log plot of the thermal-lens signal calculated by the linear model, Eq. (3) and Shen–Snook equation, Eq. (2), on the excitation power, water. Setup, TLS-60; Geometry constant *B*, Eq. (4), 0.72; Sample absorbance, 0.002.

Tables

Table S1. Silicon oxide LUDOX grades AM, SM-30, CL-X, TMA, HS-40, TM-50, GRACE, USA, the characteristics provided by the manufacturer

Parameter	Brand					
	AM	**SM-30**	**CL-X**	**TMA**	**HS-40**	**TM-50**
Particle charge	Negative					
Average particle diameter, nm	12	7	22	22	12	34
Silica gel (according to SiO_2), % w/w	30	30	45	34	40	50
pH (25°C)	8.9	10.0	9.1	9.0	9.7	9.0
Specific surface area, m^2/g	220	345	130	140	220	140
Titrated alkali (as Na_2O), % w/w	0.24	0.56	0.19	0.21	0.41	0.5

Table S2. Selection of coefficients of functions describing the formation and dissipation of a thermooptical element in thermal lens experiment, MetHbCN, 6.0 μmol/L (P = 0.95). Setup, TLS-60; excitation wavelength, 514.5 nm; excitation power, 40.0 mW

Equation	$y = y_0 + ae^{-bx}$			$y = y_0 + ae^{-bx} + fe^{-gx}$				
Development curve	$y_0 \times 10^{-2}$	$a \times 10^{-2}$	$b \times 10^{2}$	$y_0 \times 10^{-2}$	$a \times 10^{-2}$	$b \times 10^{2}$	$c \times 10^{-2}$	$d \times 10^{2}$
Coefficient value	5.274	17.10	5.840	0.0098	9.612	5.840	7.4902	5.840
R	< 0.0001	0.9963	0.9963	< 0.0001	1.0000	0.9991	1.0000	9.9991
Dissipation curve	$y_0 \times 10^{-10}$	$a \times 10^{-10}$	$b \times 10^{2}$	$y_0 \times 10^{-10}$	$a \times 10^{-10}$	$b \times 10^{2}$	$f \times 10^{6}$	g
Coefficient value	$<10^{-5}$	0.00047	10^{-3}	–0.381	3.8128	1.20	3.1233	0.0669
R	< 0.0001	0.9963	0.9963			<0.0001		

Procedures

Procedure S1. Determination of solubility constants of metal iodides [4].

Weighed portions of potassium iodide (0.2 g) and ascorbic acid (0.5 g) are placed into a 50-mL volumetric flask. The solution is diluted to the mark with doubly distilled deionized water. A 2-mL portion of this solution is mixed with 0.1 mL of 1 M sulfuric acid and, next, mixed with an aliquot portion of a test metal (copper(I), copper(II), lead(II), antimony(III), or tin(II)) solution, and the solution is diluted to 5 mL with doubly distilled deionized water. The thermal lens signal is measured after 10 min at 488.0 nm. The blank is carried out similarly, but without adding the test metal solution.

Procedure S2. Preparation of solutions $Co(NO_3)_2 \times 6H_2O$.

To prepare the base solution No. 1, 5.00 g of cobalt sulfate hexahydrate $Co(NO_3)_2 \times 6H_2O$ (M = 291.03 g/mol) was placed in a measuring flask of 50.0 mL, dissolved, diluted to the label with distilled water. Similarly, for the preparation of base solution No. 2, 20.00 g $Co(NO_3)_2 \times 6H_2O$ was placed in a measuring flask of 50.0 mL. Base solutions with a concentration of 0.1 g/mL (0.344 mol/L) and 0.4 g/mL (1.374 mol/L), respectively, were prepared. Working solutions were prepared according to Table S3 in 2-mL Eppendorf polypropylene tubes.

Table S3. Compositions of working solutions $Co(NO_3)_2 \times 6H_2O$

Volume of base solution No1, μl	100	200	300	400	500	600	700	800
Water volume, μl	1900	1800	1700	1600	1500	1400	1300	1200
Volume of base solution No1, μl	900	1000	1100	1200	1400	1600	1800	2000
Water volume, μl	1100	1000	900	800	600	400	200	0
Volume of base solution No2, μl	600	700	800	900	1000	1400	1800	–
Water volume, μl	1900	1800	1700	1600	1500	1400	1300	–

Procedure S3. Preparation of gentian violet solutions.

To prepare the base solution, 50 mg of gentian violet, $C_{25}H_{30}N_3Cl$ (M = 407.979 g/mol) was placed in a measuring flask of 50.0 mL, dissolved, the solution was diluted to the mark with distilled water, thus, a solution with a concentration of 1 mg/mL (2.451 mmol/L) was prepared. Working solutions were prepared according to Table S4 in 2-mL Eppendorf polypropylene tubes.

Table S4. Compositions of working solutions of gentian violet

Volume of base solution, μl	1	5	10	20	30	40	50	60	70
Water volume, μl	1999	1995	1990	1980	1970	1960	1950	1940	1930
Volume of base solution, μl	80	90	100	120	140	180	200	220	260
Water volume, μl	1920	1910	1900	1880	1860	1820	1800	1780	1740
Volume of base solution, μl	300	400	500	600	700	800	900	1000	2000
Water volume, μl	1700	1600	1500	1400	1300	1200	1100	1000	0

Procedure S4. Preparation of ferroin solutions.

To prepare the base solution, 50 mg of ferroin (M = 692.52 g/mol) was placed in a measuring flask of 50.0 mL, dissolved, the solution was diluted to the mark with distilled water, thus, a solution with a concentration of 1 mg/mL (1.444 mmol/L) was prepared. Working solutions were prepared according to Table S5 in 2-mL Eppendorf polypropylene tubes.

Table S5. Compositions of ferroin working solutions

Volume of base solution, µl	10	20	30	40	50	60	70	80	90	100	150	200
Water volume, µl	1990	1980	1970	1960	1950	1940	1930	1920	1910	1900	1850	1800
Volume of base solution, µl	250	300	350	400	450	500	550	600	650	700	750	800
Water volume, µl	1750	1700	1650	1600	1550	1500	1450	1400	1350	1300	1250	1200

Procedure S5. Preparation of nanodiamond solutions for spectrophotometric measurements.

The base solution of nanodiamonds was prepared as given in [5,6]. If the age of the base solution was more than a day, then before preparing working solutions, the base solution was thoroughly mixed with intensive manual shaking and voiced in the bath for an hour. Then a series of working solutions was prepared according to Table S6 in 2-mL Eppendorf polypropylene tubes.

Table S6. Compositions of working solutions of nanodiamonds for spectrophotometric measurements

Volume of base solution, µl	10	200	300	400	500	600	700	800	900	1000
Water volume, µl	1900	1800	1700	1600	1500	1400	1300	1200	1100	1000
Volume of base solution, µl	1100	1200	1300	1400	1500	1600	1700	1800	1900	2000
Water volume, µl	900	800	700	600	500	400	300	200	100	0

Procedure S6. Aqueous solutions of surfactants.

For each test solution of surfactants at each concentration indicated in the second column, a series of 6 solutions containing the colored substance specified in the third column in the corresponding (column 4) concentration range was prepared (Table S7). The solutions were prepared in such a way that the sixth solution did not contain a colored substance, and in the remaining five its concentrations changed evenly over the specified range. All solutions were prepared in measuring flasks of 25 mL and brought to a mark at 20°C doubly distilled water. After homogenization in a Branson ultrasonic bath, 10 min were allowed to settle for 3 min. After making sure of the homogeneity of the solution, thermal-lens determination was carried out on spectrometer No. 1 at λ_e = 488.0 nm (in the case of ammonium dichromate) and at λ_e = 514.5 nm (in the case *of tris).* (2-nitroso-1-naphtholate) cobalt(III)) at the excitation radiation power P_e = 40 mW for 3-5 min, and also measured the optical density of all solutions at wavelengths of 488 nm and 514 nm respectively relative to surfactant solutions in doubly distilled water of the appropriate concentration.

Table S7. Concentration of working solutions of surfactants and colorants

Surfactants	Concentration, % wt.	Colorant	Colorant concentration range, mol/l
Brij–35	0.25; 0.5; 0.75; 1.0; 1.5; 2.0; 2.5; 5.0; 10	Ammonium dichromate; tris-(2-nitroso-1-naphtholate) cobalt(III)	$5 \cdot 10^{-5}$–$4.2 \cdot 10^{-4}$ $3 \cdot 10^{-7}$–$2 \cdot 10^{-5}$
Triton–X100	0.25; 0.5; 1.0; 1.5; 2.0; 2.5; 5.0; 10	Ammonium dichromate; tris-(2-nitroso-1-naphtholate) cobalt(III)	$5 \cdot 10^{-5}$–$4.2 \cdot 10^{-4}$ $3 \cdot 10^{-7}$–$2 \cdot 10^{-5}$
Tween–80	0.25; 0.5; 1.0; 1.5; 2.0; 2.5; 5.0; 10	Ammonium dichromate; tris-(2-nitroso-1-naphtholate) cobalt(III)	$5 \cdot 10^{-5}$–$4.2 \cdot 10^{-4}$ $3 \cdot 10^{-7}$–$2 \cdot 10^{-5}$
Sodium dodecyl sulfate	0.25; 0.5; 0.75; 1.0; 1.25; 1.5; 2.0; 2.5	Ammonium dichromate	$8 \cdot 10^{-5}$–$9 \cdot 10^{-4}$.

References

1. Tishchenko, K.; Muratova, M.; Volkov, D.; Filichkina, V.; Nedosekin, D.; Zharov, V.; Proskurnin, M. Multi-wavelength thermal-lens spectrometry for high-accuracy measurements of absorptivities and quantum yields of photodegradation of a hemoprotein–lipid complex. *Arab. J. Chem,* **2017**, *10*, 781-791, doi:10.1016/j.arabjc.2016.01.009.
2. Shen, J.; Lowe, R.D.; Snook, R.D. A model for cw laser induced mode-mismatched dual-beam thermal lens spectrometry. *Chem. Phys.* **1992**, *165*, 385-396, doi:10.1016/0301-0104(92)87053-c.
3. Baesso, M.L.; Shen, J.; Snook, R.D. Time-resolved thermal lens measurement of thermal diffusivity of soda—lime glass. *Chem. Phys. Lett.* **1992**, *197*, 255-258, doi:10.1016/0009-2614(92)85764-2.
4. Chernysh, V.V.; Nesterova, I.V.; Proskurnin, M.A. The studies of the reaction of bismuth(III) with iodide at nanogram level by thermal lensing. *Talanta* **2001**, *53*, 1073-1082, doi:https://doi.org/10.1016/S0039-9140(00)00603-2.
5. Usoltseva, L.O.; Volkov, D.S.; Karpushkin, E.A.; Korobov, M.V.; Proskurnin, M.A. Thermal Conductivity of Detonation Nanodiamond Hydrogels and Hydrosols by Direct Heat Flux Measurements. *Gels* **2021**, *7*, 248.
6. Proskurnin, M.A.; Usoltseva, L.O.; Volkov, D.S.; Nedosekin, D.A.; Korobov, M.V.; Zharov, V.P. Photothermal and Heat-Transfer Properties of Aqueous Detonation Nanodiamonds by Photothermal Microscopy and Transient Spectroscopy. *J. Phys. Chem. C* **2021**, *125*, 7808-7823, doi:10.1021/acs.jpcc.0c09329.